UC Santa Barbara
UC Santa Barbara Previously Published Works

Title

Global load-sharing model for unidirectional hybrid fibre-reinforced composites

Permalink

https://escholarship.org/uc/item/6422418r

Authors

Swolfs, Yentl

McMeeking, RM

Rajan, VP

et al.

Peer reviewed

Global load-sharing model for unidirectional hybrid fibre-reinforced composites

Yentl Swolfs [a,*], R.M. McMeeking [b,c,d], V.P. Rajan [c], F.W. Zok [c], Ignaas Verpoest [a], Larissa Gorbatikh [a]

[a] Department of Materials Engineering, KU Leuven, Kasteelpark Arenberg 44 bus 2450, Belgium
[b] Department of Mechanical Engineering, University of California, Santa Barbara, CA 93106, USA
[c] Materials Department, University of California, Santa Barbara, CA 93106, USA
[d] School of Engineering, University of Aberdeen, King's College, Aberdeen AB24 3UE, Scotland, UK

ARTICLE INFO

ABSTRACT

A promising strategy to increase the tensile failure strain of carbon fibre-reinforced composites is to hybridise carbon fibres with other, higher-elongation fibres. The resulting increase in failure strain is known as the hybrid effect. In the present article, a global load-sharing model for hybrid composites is developed and used to carry out a parametric study for carbon/glass hybrids. Hybrid effects of up to 15% increase in failure strain are predicted, corresponding reasonably well to literature data. Scatter in the carbon fibre strength is shown to be crucial for the hybrid effect, while the scatter in glass fibre strength is much less important. In contrast to reports in earlier literature, the ratio of failure strains of the two fibres has only a small influence on the hybrid effect. The results provide guidelines for designing optimal hybrid composites.

© 2015 Elsevier Ltd. All rights reserved.

1. Introduction

Carbon fibre-reinforced polymer matrix composites combine excellent mechanical properties with low density, making them a popular choice for lightweight, high-performance applications (Verpoest et al., 2014). Among their main limitations are their low tensile failure strain (only about 2%) and their high cost. Higher failure strains can be obtained with the use of polymer fibres (Swolfs et al., 2013a, 2014c, 2014d) or metal fibres (Callens et al., 2014), but these changes are accompanied by reductions in stiffness and strength and/or an increase in density.

An alternative solution is to employ hybridisation, wherein two fibre types are combined in a single composite. By hybridising, the drawbacks of one fibre can be balanced out by the virtues of the other (Hine et al., 2014; Swolfs et al., 2014a). The most common combination is carbon and glass: carbon being the low-elongation fibre (LE) and glass the high-elongation (HE) fibre. This hybrid composite maintains good mechanical performance but dramatically reduces the cost compared to an all-carbon fibre-reinforced composite. Furthermore, some hybrid composites are known to exhibit synergistic effects whereby their properties exceed those expected based on considerations of rules-of-mixtures (Czél and

Wisnom, 2013; Diao et al., 2012; Kretsis, 1987; Manders and Bader, 1981; Peijs et al., 1990; Perry and Adams, 1975; Swolfs et al., 2014b; Taketa et al., 2010; You et al., 2007). This is referred to as the hybrid effect.

Hayashi (1972) is credited with the discovery of the hybrid effect. Hayashi found that the failure strain of an all-carbon fibre composite could be increased by 40% by sandwiching the carbon fibre layers between glass fibre layers. Despite some confusion among early researchers, as documented by Phillips (1976), the hybrid effect in regard to initial failure strain is now well established. Three main causes quoted for the hybrid effect are (1) residual thermal stresses, (2) fracture propagation effects, and (3) dynamic stress concentrations (Swolfs et al., 2014b).

Residual stresses are caused by differences in thermal expansion coefficients of the two fibre types. They arise upon cooling following curing of a thermosetting resin or solidification of a thermoplastic resin. They lead to residual axial compressive stresses in the carbon fibres, which counteract the applied stresses and lead to an apparent failure strain enhancement (Manders and Bader, 1981). Using representative thermal expansion coefficients and longitudinal Young's moduli, the magnitude of this hybrid effect can be shown to be small for carbon/glass hybrid composites.

The second cause, the fracture propagation effect, is based on the way unidirectional composites fail. Being brittle, fibres do not have a deterministic strength, but rather have strengths that follow weakest link fracture statistics. When a fibre breaks in a composite, the surrounding matrix is loaded in shear. The matrix transfers stress to the intact segment of the broken fibre through shear lag. Simultaneously, the shear in the matrix transfers load shed by the broken fibre onto those surrounding it. The resulting stress concentrations in surrounding fibres increase their failure probability (Behzadi et al., 2009; Nedele and Wisnom, 1994; Swolfs et al., 2013b) and eventually leads to the development of clusters of spatially-correlated broken fibres (Pimenta and Pinho, 2013; Scott et al., 2012; Swolfs et al., 2015b, 2015d). Once a cluster reaches a critical size, additional fibre fracture occurs unstably and the composite ruptures.

Hybridisation can influence the fibre failure process in several ways. Firstly, stress concentrations and stress recovery at a broken fibre are altered by the presence of neighbouring fibres with different stiffness (Swolfs et al., 2013c; Zweben, 1977). Because of the dynamic nature of fibre fracture, changes in the local elastic moduli also alter the propagation of the resulting stress waves (Xing et al., 1981). Secondly, if the two fibre types are dispersed uniformly, the development of a critical cluster of the LE fibres may be delayed by the presence of the neighbouring HE fibres (Harlow, 1983). Finally, a point often overlooked, scaling effects also play a role. For a constant sample size, the number of LE fibres is reduced by hybridisation. A composite with fewer LE fibres has a higher probability of reaching high strengths. The magnitude of this effect is presently not known.

Dynamic stress concentrations (Xing et al., 1981) and thermal stresses (Manders and Bader, 1981) have been judged to be insufficient to rationalise the reported magnitudes of the hybrid effects (typically 10–50%) (Kretsis, 1987). Therefore, it is generally assumed that the fracture propagation effect is the dominant cause.

Many authors have attempted to model hybrid composites (Dai and Mishnaevsky, 2014; Fukuda, 1984; Fukunaga et al., 1984; Swolfs et al., 2015a; Zeng, 1994; Zweben, 1977) Several of the influencing parameters have been analysed, but the conclusions are not always straightforward to interpret. Zweben (1977) indicated that the ratio of the failure strain for the two fibre types is a critical parameter controlling the hybrid effect, while Fukuda (1984) later showed that this does not influence the hybrid effect. This apparent disagreement, however, was based on differing definitions of the hybrid effect.

Fukunaga et al. (1984) demonstrated that the hybrid effect is equal to zero if the LE fibres have a deterministic strength. From a theoretical viewpoint, it can indeed be deduced that in this situation the fracture propagation effect vanishes. However, the converse effect – a potential change in failure strain due to high scatter in the strengths of the HE fibres – has not been proven or demonstrated.

Models of fibre fragmentation and bundle rupture for composites with a single fibre population are well established. A useful baseline of results is obtained by assuming that stress re-distribution around fibre breaks follows global load-sharing (GLS). This approach assumes that the load shed by a broken fibre is distributed uniformly over all unbroken fibres in the plane of the break (Curtin, 1991a, 1991b). Under these conditions, the fibres break independently of one another. Although such models normally neglect the axial stress borne by the matrix, the matrix contribution can be added to the bundle response in a straightforward manner.

Curtin was the first to develop an approximate analysis of the stress–strain response of a fragmenting bundle. Assuming that the fibre strength follows a Weibull distribution and using a Taylor series expansion to approximate the Weibull function, Curtin obtained useful analytic solutions for the stress–strain curve as well as the strength and failure strain. Curtin's model was later extended by Neumeister to account in an approximate way for the overlap of influence zones adjacent to fibre breaks (Neumeister, 1993a, 1993b). Hui et al. (1995) subsequently developed an exact solution to the fibre fragmentation problem.

The principal objective of the present article is to develop a GLS framework for predicting tensile failure of hybrid composites, based on Hui's exact fibre fragmentation solution (Hui et al., 1995). A parametric study is conducted on a family of hybrid composites comprising carbon and glass fibres in an epoxy matrix. The framework presented here could be readily adapted to other fibre combinations. Some of the limitations of the GLS approach are discussed in due course.

2. Model description

2.1. Assumptions

The exact solution of the fibre fragmentation process was developed by Hui et al. (1995). The key analytic results needed for the analysis are presented in Appendix A. A synopsis of the nature of the model and the underlying assumptions follows. The assumptions in the model are broadly consistent with those employed by many others in the analysis of fibre bundle fracture.

The statistical variation of fibre strength is assumed to follow a Weibull distribution:

$$P = 1 - \exp\left(-\frac{L}{L_0}\cdot\left(\frac{\sigma_f}{\sigma_0}\right)^m\right)$$

(1)

where P is the cumulative failure probability of a fibre with gauge length L at a longitudinal fibre stress σ_f, m the Weibull modulus, σ_0 the Weibull scale parameter and L_0 the characteristic length. Although its dependence on stress is empirical, the Weibull function is recognised as being the simplest one that captures the strength distribution of many brittle materials. Other, more complex distributions have been proposed (Curtin, 2000; Swolfs et al., 2015c; Thomason, 2013; Watanabe et al., 2014) and could in principle be used in conjunction with the present analysis. But these functions result in additional fitting parameters that do not necessarily provide additional insight into the mechanics and physics of fibre bundle fracture. They are therefore not employed here.

The model further assumes that, when a fibre breaks, the load it carried before breaking is shed equally to all other fibres in the plane of the break: the so-called global load sharing condition. Consequently, each fibre is only influenced by the other fibres through the average response of the matrix and all other fibres. Since the model does not take into account local effects, the spatial distribution of the fibres is irrelevant.

The stress in the broken fibre progressively builds up on either side of the break by a shear transfer process within the break influence zone. This is the region in which the fibre stress is less than that in remote locations. The latter stress corresponds to the axial composite strain times Young's modulus of the fibre. Shear transfer occurs either through frictional sliding following interfacial debonding or through matrix shear yielding. Frictional sliding is typical in ceramic matrix composites, whereas matrix yielding is more common in polymer matrix composites and in some metal–matrix composites. That which occurs is irrelevant to the model, provided the resulting shear stress τ_0 is uniform throughout the break influence zone. The assumption of a constant shear stress has been investigated by others for cases in which shear transfer occurs through matrix yielding. Notably, Landis and McMeeking (1999) found that the assumption of constant shear stress is reasonable if the fibre stress is much larger than the shear yield stress of the matrix. de Morais (2006) reached a similar conclusion and pointed out that uncertainties in the constituent property data are unlikely to justify use of a more complex shear stress distribution.

The model is further based on the assumption that the length of the break influence zone is small compared to the gauge length of the tested material. The analysis proceeds by computing the probability density of fragments of various lengths and the average stress borne by these fragments, incorporating the effects arising from overlapping break influence zones as well as "shadowing" of prospective defects by existing breaks. Such effects become important in properly capturing the softening behaviour in the post-peak domain (Rajan and Zok, 2012). This softening is crucial to failure of the hybrid composites: a feature that will be brought out by the forthcoming results.

Finally, the model assumes the presence of essentially an infinite number of fibres, thereby allowing the use of a continuous failure distribution function. It is recognised that, when the number of fibres is finite, the composite strength is no longer deterministic and exhibits a weak dependence on specimen size (Ibnabdeljalil and Curtin, 1997; Phoenix et al., 1997; Pimenta and Pinho, 2013). Such size scaling effects are neglected in the present analysis.

The results are cast in terms of normalised strain and stress quantities, defined by

$$\Delta = \frac{\varepsilon E_f}{\sigma_{char}},$$

(2)

$$S = \frac{\bar{\sigma}}{V_f \sigma_{char}},$$

(3)

where ε is the applied strain, E_f is the longitudinal Young's modulus of the fibre, $\bar{\sigma}$ is the average composite stress, V_f is the fibre volume fraction, and σ_{char} is a characteristic strength, defined by

$$\sigma_{char} = \sigma_0{}^m\left(\frac{\tau_0\cdot L_0}{\sigma_0\cdot R}\right)^{1/m+1}$$

(4)

with R being the fibre radius. The fragmentation analysis is couched in terms of σ_{char} and a characteristic stress transfer length δ_{char}, defined by

$$\delta_{char} = L_0 \left(\frac{R \cdot \sigma_0}{\tau_0 \cdot L_0} \right)^{m/m+1},$$

(5)

Using typical property values in Eq. (5), it is readily shown that δ_{char} is about two orders of magnitude smaller than the lengths typically used for measuring fibre and composite strengths.

2.2. Extension to hybrid composites

Since the GLS model does not take into account local effects, the spatial distribution of the two fibre populations is irrelevant. That is, it does not matter whether the two fibre types are segregated or well mingled. Thus, in adapting the GLS model, the hybrid composite is conceptually split up into two parallel sub-composites: one containing all of the LE fibres and the other with all of the HE fibres. Consequently, the overall response is calculated from a volumetric averaging based on the relative fractions of the two fibre types and assuming equal axial strains. The homogenised stress $\bar{\sigma}_H$ of the hybrid composite therefore becomes

$$\bar{\sigma}_H(\varepsilon) = \bar{\sigma}_{LE}(\varepsilon) V_{f,LE} + \bar{\sigma}_{HE}(\varepsilon) V_{f,HE}$$

(6)

where $\bar{\sigma}_{LE}$ and $\bar{\sigma}_{HE}$ are the average stresses in the LE and HE fibre sub-composites, respectively, and $V_{f,LE}$ and $V_{f,LE}$ are the relative volume fractions of LE and HE fibre sub-composites, respectively. The sum of $V_{f,LE}$ and $V_{f,HE}$ is equal to 1. The volume fraction of the matrix within each sub-composite is taken into account through the calculation of $\bar{\sigma}_{LE}$ and $\bar{\sigma}_{HE}$. The calculation of $\bar{\sigma}_{LE}$ and $\bar{\sigma}_{HE}$ proceeds in the manner described in the Appendix.

The composite is assumed to fail when the stress–strain curve first reaches a maximum. This corresponds to the tangent modulus reaching zero. Differentiating Eq. (6), setting the tangent modulus equal to zero, and non-dimensionalising stress and strain in accordance with Eqs. ((2) and 3) yields the condition

$$V_{f,LE} E_{f,LE} \left[\frac{dS_{LE}(m_{LE}, \Delta_{LE})}{d\Delta_{LE}} \right] + V_{f,HE} E_{f,HE} \left[\frac{dS_{HE}(m_{HE}, \Delta_{HE})}{d\Delta_{HE}} \right] = 0$$

(7)

Since the strains in the LE and HE fibre composites are identical, it follows from Eq. (2) that

$$\varepsilon = \frac{\Delta_{LE} \sigma_{char,LE}}{E_{f,LE}} = \frac{\Delta_{HE} \sigma_{char,HE}}{E_{f,HE}}.$$

(8)

This result can be rewritten non-dimensionally as

$$\Delta_{HE} = \bar{\sigma}_{ND} \Delta_{LE}$$

(9)

where

$$\bar{\sigma}_{ND} = \frac{\sigma_{char,LE} E_{f,HE}}{\sigma_{char,HE} E_{f,LE}}$$

(10)

Next, a non-dimensional stiffness parameter, $\bar{E}_{ND}$, is introduced:

$$\bar{E}_{ND} = \frac{E_{f,LE} \cdot V_{f,LE}}{E_{f,HE} \cdot V_{f,HE}}$$

(11)

Combining Eqs. (7)–(11) leads to the final expression:

$$\bar{\sigma}_{ND} \bar{E}_{ND} \left[\frac{dS_{LE}(m_{LE}, \Delta_{LE})}{d\Delta_{LE}} \right] + \left[\frac{dS_{LE}(m_{HE}, \bar{\sigma}_{ND} \Delta_{LE})}{d\Delta_{LE}} \right] = 0$$

(12)

The solution to this equation leads to the failure strain of the LE sub-composite $\Delta_{LE,H}^{failure}$ in the hybrid composite. It depends on four parameters: m_{LE}, m_{HE}, $\bar{E}_{ND}$ and $\bar{\sigma}_{ND}$. The failure strain of the LE fibre composite $\Delta_{LE}^{failure}$ serves as a reference, and only depends on m_{LE}. The hybrid effect H^{effect} is defined as the failure strain increase relative to that of the LE fibre composite, given by

$$H^{effect} = \frac{\Delta_{LE,H}^{failure} - \Delta_{LE}^{failure}}{\Delta_{LE}^{failure}}$$

(13)

A similar definition can also be set up in terms of dimensional strains ε instead of non-dimensional strains Δ. It should be emphasised that $\Delta_{LE,H}^{failure}$ in this case is the failure strain of the carbon fibre sub-composite in the hybrid composite, and not the overall failure strain. The failure strain of the carbon fibre sub-composite corresponds to the strain at which the tangent modulus is zero for the first time. This definition therefore complies with the definition proposed in a recent review paper on hybrid composites (Swolfs et al., 2014b).

A useful limiting case to consider is the one in which the HE fibre composite exhibits minimal non-linearity when the hybrid composite fails. In this case, the second term in brackets in Eq. (12) reduces to $\bar{\sigma}_{ND}$, and the failure condition becomes

$$\bar{E}_{ND}\left[\frac{dS_{LE}(m_{LE}, \Delta_{LE})}{d\Delta_{LE}}\right] + 1 = 0 \tag{14}$$

In this limit, the hybrid effect depends only on $\bar{E}_{ND}$ and m_{LE}. This illustrates the usefulness of this non-dimensional analysis in gaining insight into the parameters governing the hybrid effect.

It should be emphasised that the GLS approach has several implications in the predictions of the hybrid effect. Firstly, as noted previously, the dispersion of the two fibre types is tacitly neglected, though such effects have been observed in some hybrid systems (Kretsis, 1987; Swolfs et al., 2014b). These effects can only be addressed through a local load sharing model. Such a model has been developed and was presented elsewhere (Swolfs et al., 2015a). Secondly, contributions from residual thermal stresses and dynamic effects are ignored. Adding residual stresses to the model would be straightforward, though such effects are expected to have a minor influence on the results (Manders and Bader, 1981; Zweben, 1977). Little is known in literature about the dynamic effect, making it difficult to judge its importance (Swolfs et al., 2014b; Xing et al., 1981). Finally, delaminations between the LE and HE fibre layers are ignored. This would not affect the hybrid effect, as this is defined based on the first failure of the LE composite. It would however affect the appearance of the stress–strain diagrams after this first failure. The more refined model developed by the present authors could potentially be used for such an analysis, but does not include delaminations yet (Swolfs et al., 2015a).

2.3. Material input data

The parametric study focuses on carbon/glass epoxy hybrid composites, since these have been the systems most commonly investigated. Parameters referring to LE carbon fibres will be indicated with subscript *CF*, while subscript *GF* is used for the HE glass fibres. The overall fibre volume fraction in each of the two composite types is taken to be 50%, although this value does not affect the failure strain.

The reported Weibull strength parameters for the two fibre types vary over a wide range (Naito et al., 2008; Wang et al., 2010; Watanabe et al., 2013). For the purpose of the parametric study, the values were chosen to be those typically quoted by the fibre manufacturers: $\sigma_{0,CF} = 5000$ MPa, $m_{CF} = 7$ and $L_{0,CF} = 25$ mm for carbon fibre and $\sigma_{0,GF} = 2500$ MPa, $m_{GF} = 7$ and $L_{0,GF} = 25$ mm for glass fibre. Because the hybrid effect is defined as a relative failure strain enhancement, the exact values of the Weibull parameters prove to be relatively unimportant. The longitudinal fibre moduli were $E_{f,CF} = 230$ GPa and $E_{f,GF} = 70$ GPa, and the matrix shear yield stress, τ_0, was 50 MPa. The fibre radii, R_{CF} and R_{GF} are 3.5 μm and 6 μm respectively. Some of these parameters will be varied to assess their importance in the hybrid effect. Such variations will be clearly indicated when results are presented below.

3. Results and discussion

3.1. Effects of glass fibre volume fraction

The hybrid volume fraction is crucial to the hybrid effect. There is considerable experimental evidence showing that
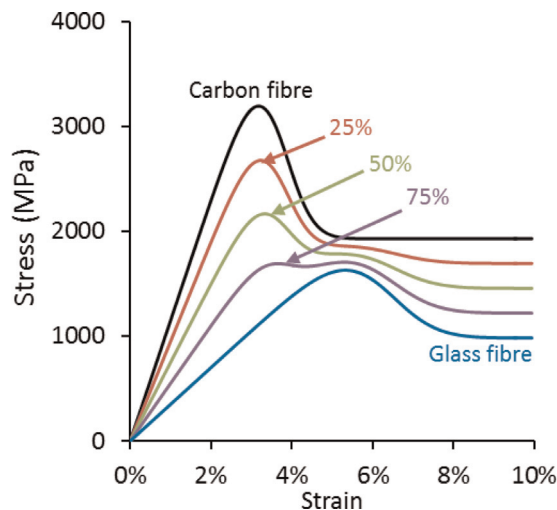

Fig. 1. Predicted stress–strain curves of the two reference composites and three hybrid composites, with their hybrid volume fractions, $V_{f,GF}$, indicated.
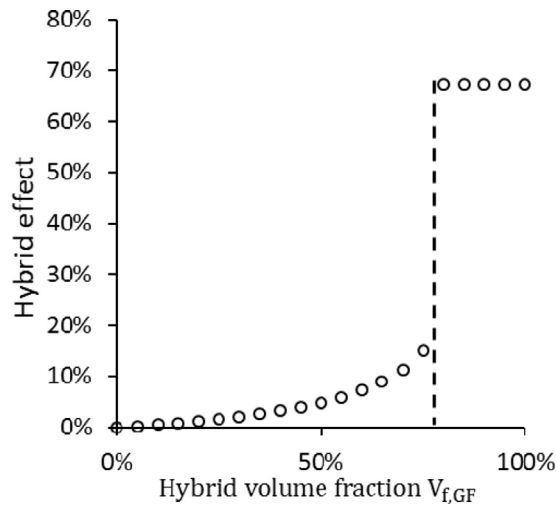
Fig. 2. The hybrid effect as a function of the hybrid volume fraction. The dashed line represents the hybrid volume fraction beyond which the failure strain is controlled entirely by that of the glass fibres.

larger hybrid effects are obtained at higher volume fractions of HE fibres (Kretsis, 1987).

Stress–strain diagrams for three hybrids as well as those for the two reference composites are plotted in Fig. 1. For non-hybrid composites, Hui's model captures the post-peak softening and the transition into a plateau. In the plateau region, the fibre fragment lengths are below the critical length at which additional stress can build up via shear lag and hence no additional fibre fracture can occur. In reality, at very large strains, the stress will begin to decrease below the plateau level as the composite pulls apart. Since the strains at which composite failure occurs in the hybrid composites is only slightly larger than the failure strain of the LE fibres, the effects of this further softening at very large strains is not expected to be important.

The softening regime may significantly contribute to the hybrid effect. Although the softening cannot be exploited in uniaxial tension tests of composites with a single Weibull flaw population, it represents the crucial element in enabling the hybrid effect in composites with two disparate distributions in failure strains.

The tensile strength here is defined as the maximum in the stress–strain curve and the corresponding tensile strain is taken to be the failure strain. With these definitions, the reference carbon fibre composite has a strength of 3193 MPa and a failure strain of 3.17%, while these parameters are 1627 MPa and 5.33% respectively for the reference glass fibre composite. The predicted failure strains exceed the values measured experimentally by a significant margin. Typically, measured failure strains are 1.5–2.0% and 2.5–3.5% for the carbon and glass fibre composites, respectively. The discrepancies are likely due to the neglect of stress concentrations in the current GLS model. More importantly, the predicted ratio of failure strains (about 0.6) corresponds well with that measured experimentally. The expectation thus is that, because of the way in which it is defined, the predicted hybrid effect should be pertinent to the real composites.

As the volume fraction of glass fibres is increased, the strength of the hybrid composite decreases whereas its initial failure strain gradually increases. This enhancement in failure strain or hybrid effect (see Fig. 1) is attributable largely to the finite (and still rather high) tangent modulus of the glass fibre composite at the point at which the carbon fibre composite is rounding its peak and beginning to soften. Beyond a critical volume fraction ($V_{f,GF} \approx 80\%$) the peak in the stress–strain curve that is controlled by the carbon fibres at lower $V_{f,GF}$ values is replaced by a "shoulder" in the curve. The peak in this domain is controlled entirely by the failure strain of the glass fibres, independent of $V_{f,GF}$. Although the increase in failure strain is substantial, it is not considered to be a hybrid effect in the way the term has been defined here.

A similar bimodal stress–strain diagram was also found in Phoenix (1974). A similar, but smaller hybrid effect can be seen in this work. Phoenix used the equal load sharing principle of Rosen (1964), which means a fibre stops carrying load over its entire length when it breaks. In contrast, the global load sharing model allows a broken fibre to recover its load carrying capability through friction or shear stress transfer in the matrix. The main difference, however, is that Phoenix used a Weibull modulus of 20 for both fibre types. This value was chosen to represent high-performance polymer fibres, but is unrealistically high for carbon fibres. As will be shown in the next section, such a high Weibull modulus will cause a smaller hybrid effect.

Even though the GLS model does not take into account any local effects, it still predicts hybrid effects of up to 15%. These effects can be attributed to a size scaling effect, but from a somewhat unconventional source. Conventional size scaling deals with changes in strength or failure strain when either the number of fibres or their length change. Since GLS is a mean field theory, it tacitly assumes an infinite number of fibres. At each strain, the same percentage of the carbon fibres is broken in each hybrid, but higher HE volume fractions reduce the overall percentage of broken fibres. Therefore, the stress that is shed onto the HE fibres is lower and further carbon fibre failure is delayed. This is not a size scaling effect in the conventional
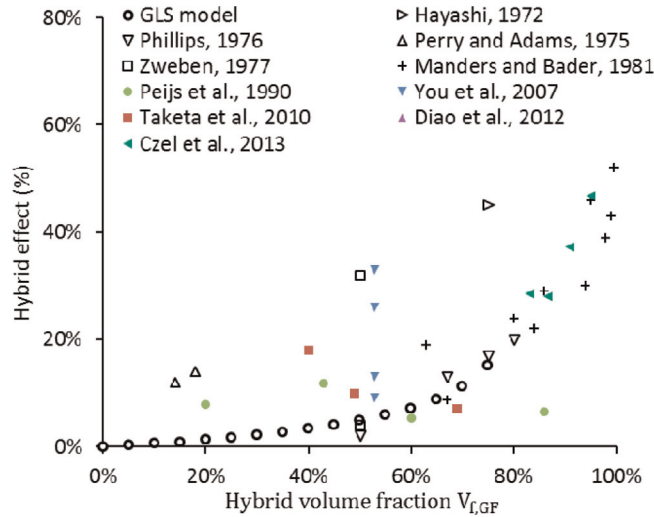
Fig. 3. Comparison of the hybrid effect predicted by GLS with experimental data available in literature.

manner, as the GLS model does not have an absolute number of fibres.

The predictions are compared with experimental data available in the literature, see Fig. 3. From this comparison, it appears that the predictions provide a reasonable representation of the experimental results, albeit at the lower end of the measured values. Some of the discrepancies are likely due to varying degrees of mixing of both fibre types, as observed in the data from You et al. (2007).

Hybridisation also influences tensile strength. Fig. 4 shows the strength of the hybrid composites as a function of the hybrid volume fraction $V_{f,GF}$. Here an additional hybrid effect can be defined, based on the difference between the strength predicted by the model and that obtained from a bi-linear rule-of-mixtures. The rule-of-mixtures is calculated in accordance with procedures described elsewhere (Kretsis, 1987; Manders and Bader, 1981; Shan and Liao, 2002). The procedure assumes that the two types of fibre act independently. Points A and B in Fig. 4 correspond to the strength of the two reference composites. Line AC represents a linear rule-of-mixtures between the carbon fibre sub-composite strength and the stress that the glass fibre sub-composite carries at the failure strain of the carbon fibres. From D to C however, the stress required to fail the carbon fibre sub-composite is insufficient to cause failure of the entire hybrid composite. In this regime, the glass fibre sub-composite requires a higher stress to fail. The strength is therefore governed by the line BD, which represents the glass fibre behaviour on its own. The overall strength envelope therefore becomes ADB. The lowest strength is expected at point D, corresponding to a hybrid volume fraction, $V_{f,GF}$, of 86%.

The present model predictions follow the bi-linear rule-of-mixtures well, apart from some deviations at high hybrid volume fractions. Notably, in contrast to the rule-of-mixtures, a strength minimum is not obtained. The absence of a strength minimum is due to the somewhat gradual softening in the post-peak domain as well as the limiting plateau stress
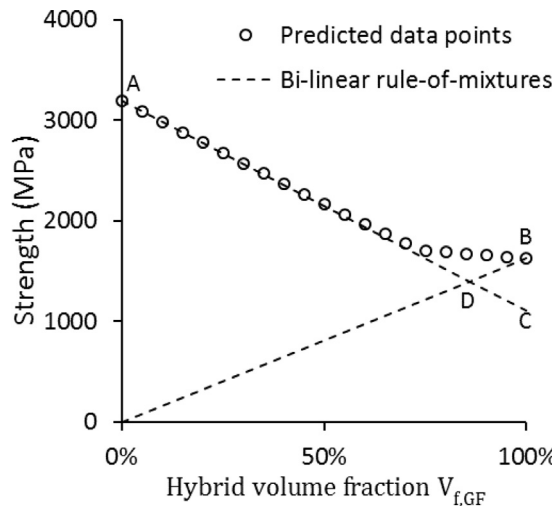

Fig. 4. The hybrid effect for strength, compared with the bi-linear rule-of-mixtures.
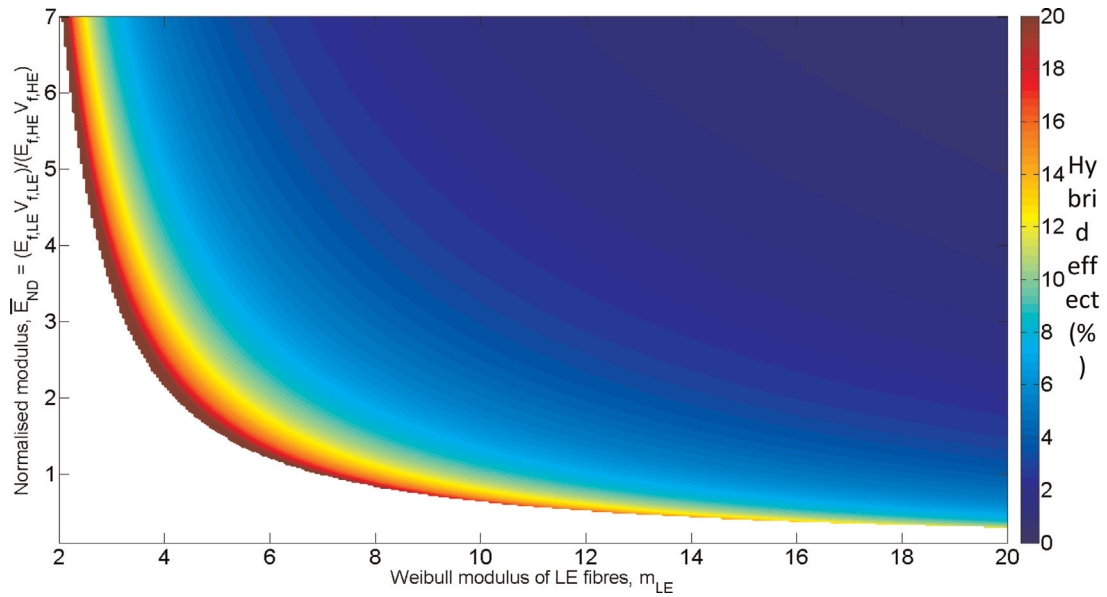
Fig. 5. Contour plot for the hybrid effect as a function of the Weibull modulus of the LE fibre and the normalised modulus, under the assumption that the HE fibres remain linear elastic. Values above 20% are topped off.

in the stress–strain response of the carbon fibre reference composite. Although highly fragmented in this domain, the carbon fibres continue to carry stress.

It should be emphasised that the proposed GLS model is essentially a "rule-of-mixtures"-model of the stress–strain diagrams predicted by Hui's model. In this regard, it is a more advanced rule-of-mixtures than the linear-elastic approximations used to set up the bi-linear rule-of-mixtures in Fig. 4.

3.2. Effects of fibre strength scatter

The preceding numerical examples reveal that the LE composite strength is attained at strains that are well below the failure strain of the HE fibres. Consequently, the degree of non-linearity in the stress–strain response of the HE fibre composite is negligible. For this limiting scenario, it is instructive to consider the solution for the failure strain of a hybrid
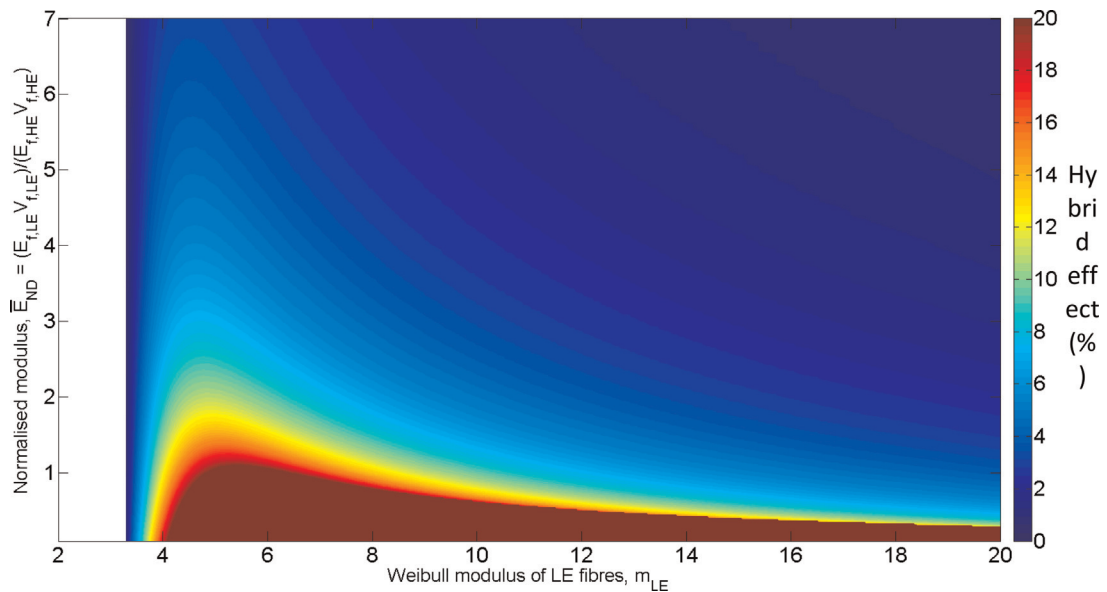

Fig. 6. Contour plot for the hybrid effect as a function of the Weibull modulus of the LE fibre and the normalised modulus, without the linear elastic assumption for the HE fibres. Values above 20% are topped off. (For interpretation of the references to color in this figure, the reader is referred to the web version of this article.)

composite with HE fibres that remain linear elastic throughout. In this limit, Eq. (14) proves that the magnitude of the hybrid effect is dictated by only two non-dimensional parameters: m_{LE} and $\bar{E}_{ND}$. Furthermore, we demonstrate below that the predictions that emerge from this limiting case are consistent with the exact results over a significant portion of the full parameter space.

Contour plots of the hybrid effect from the approximate and exact solutions are presented in Fig. 5 and Fig. 6, respectively. For the exact case, the contour plot represents a slice through the 4D space created by m_{LE}, m_{HE}, $\bar{E}_{ND}$ and $\bar{\sigma}_{ND}$. The latter plot is computed by varying the hybrid volume fraction $V_{f,HE}$, which also varies $\bar{E}_{ND}$, and m_{LE}. All the other parameters are held constant.

The white regions in these figures represent domains in which there is no solution. This can arise for two possible reasons. Firstly, in some cases LE fibre failure occurs after HE fibre failure. Secondly, the LE fibre failure is sometimes indistinguishable from the HE fibre failure. In the dark red region in Fig. 6, it was often impossible to make this distinction. This causes large, but unrealistic hybrid effects, similar to the ones observed at high hybrid volume fractions in Fig. 2. Hybrid effects above 20% are topped off to obtain a clear contour plot.

Over the domain in which solutions are attainable for both the approximate and the exact cases, the magnitudes of the hybrid effect are similar, as seen in Figs. 5 and 6. This indicates that the linear elastic assumption for the HE composite leads to accurate predictions in most cases. This conclusion also means the hybrid effect is dominated by just two parameters: m_{LE} and $\bar{E}_{ND}$.

The largest discrepancies can be found for small m_{LE} values. A small m_{LE} indicates a broad LE softening region, creating a smaller gap between the softening regions of the LE and HE composite. This will lead to reduced accuracy for the
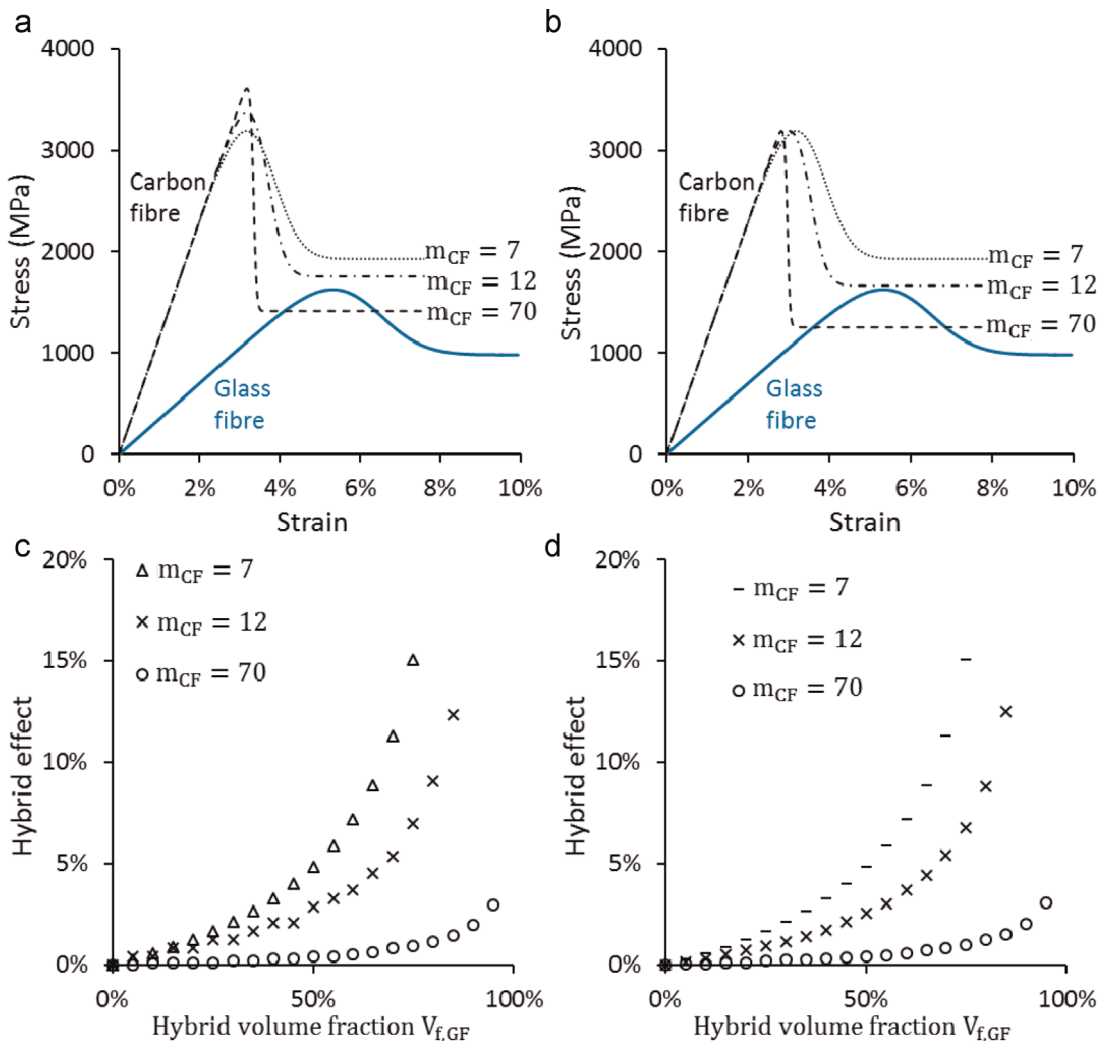

Fig. 7. Stress–strain diagrams for the reference composites with various values of the Weibull modulus, m_{CF}, for (a) the same composite failure strain, and (b) the same composite strength. The hybrid effect is plotted as a function of the hybrid volume fraction for (c) the same reference composite failure strain, and (d) the same reference composite strength.

approximate case. The hybrid effect will only be influenced by the parameters m_{HE} and $\bar{\sigma}_{ND}$ for small m_{LE} values.

Changing the hybrid volume fraction corresponds to vertical lines through the contour plot. This leads to monotonic changes in the hybrid effect, which corresponds to the trend observed in Fig. 2. Changing the Weibull modulus m_{LE} corresponds to horizontal lines through the contour plot. This change can also lead to a monotonic hybrid effect, but only in the approximate case. In the exact case, a maximum hybrid effect is observed for m_{LE} between 4 and 5. This maximum is caused by a change in the failure strain of the LE fibre reference composite. At m_{LE} below 4, the failure strain of the LE composite approaches the failure strain of the HE composite. In that case, the HE fibre composite will already start softening while the hybrid composite is failing. This reduces the failure strain of the hybrid composite. The approximate case is not valid anymore for these low m_{LE} values, as can be observed by comparing Figs. 5 and 6. The region to the left of $m_{LE}=3$ is inaccessible, since the LE fibre composite has a larger failure strain than the HE fibre composite.

These contour plots demonstrate several vital influences on the hybrid effect. Nevertheless, they have one important drawback. Changing the Weibull modulus of the LE fibres also changes the LE composite failure strain and strength. This hampers a clear separation of the observed effects from the effect of the different failure strain and strength. Changing the Weibull modulus and still maintaining the same strength or failure strain is not straightforward. It requires optimising σ_0 in such a way that the strength or failure strain are the same. This optimisation requires many runs of the models, but the efficiency of the GLS model makes this feasible. An alternative would be to use the approximation solutions for composite strength proposed by Phoenix et al. (1997). This approach would only work for the same LE composite strength, and not for the same LE composite failure strain. Therefore, an optimisation algorithm was written that finds the value of σ_0 for achieving a certain strength or failure strain. It becomes possible to investigate the influence that fibre strength scatter has on the hybrid effect. The current understanding of the fracture propagation part of the hybrid effect indicates an increased effect with increased scatter of the LE fibre strength. This feature has been previously investigated in literature, but never for constant failure strain or strength of the LE fibre composite.

The focus now shifts from general LE/HE hybrids to carbon/glass hybrids. The Weibull modulus m_{CF} of the carbon fibre strength is increased from the default value of 7 to 12 and 70. The Weibull modulus and other properties of the glass fibres are held unchanged from the values used in the previous simulations. This highest value of m_{CF}, 70, represents an unrealistically low strength scatter, which means all fibres have almost the same strength. Hereafter only exact solutions are presented.

An algorithm is implemented that changes $\sigma_{0,CF}$, while maintaining either the same failure strain or the same strength of the reference carbon fibre composite. The stress–strain curves for these two cases are plotted in Fig. 7a and b. The plateau in the stress–strain diagram occurs at lower stress levels with increased Weibull modulus. This is caused by the shorter fragments for higher Weibull moduli, which will carry a lower average stress. Furthermore, increased Weibull modulus also leads to a sharper peak.

The corresponding hybrid effects are shown in Fig. 7c and d. In all cases the hybrid effect is negligible when the Weibull modulus is very high. This is true for cases in which the reference strength or the reference failure strain are held constant, and confirms the results of Fukunaga et al. (1984).

Fig. 7c and d is proof that the hybrid effect increases for higher carbon fibre strength scatter. The results are almost the same for the two cases in which the reference failure strain or the reference strength are kept constant. Previous studies, such as Fukunaga et al. (1984), were able to prove the absence of the hybrid effect if there was no scatter on the fibre
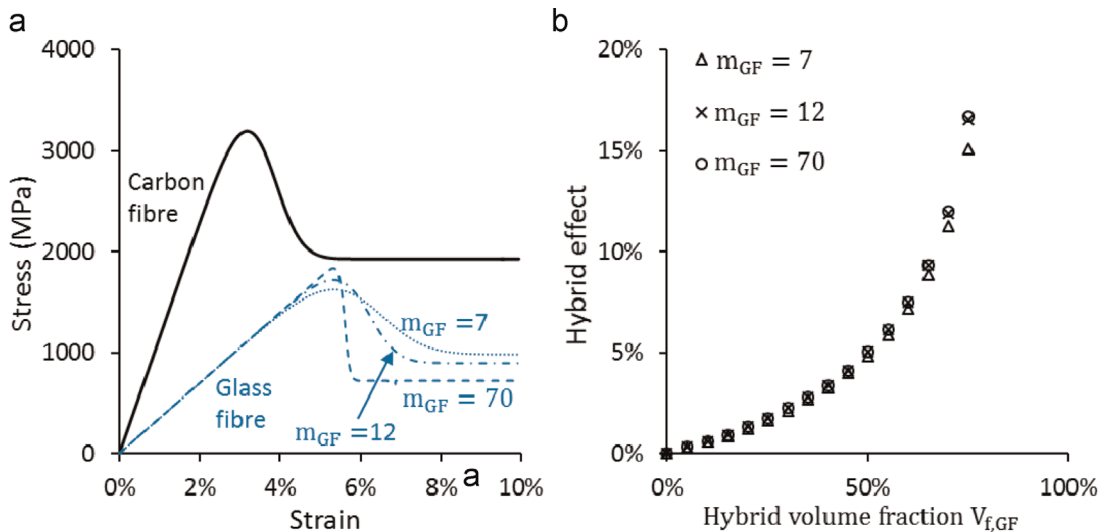

Fig. 8. (a) Stress–strain diagram of the glass fibre reference composite with various values of the glass fibre Weibull modulus, m_{GF}, when the composite failure strain is held fixed and (b) its influence on the hybrid effect.

strength of the LE fibre. Those comparisons, however, were performed without a constant baseline for the LE failure strain or strength. Since the hybrid effect is calculated compared to the reference LE fibre composite, changing the failure strain of that composite will also affect the results. These results are the first to prove this statement with a constant baseline. It also further indicates how crucial the LE fibre strength scatter is for the hybrid effect.

The results are almost the same when the reference strength and the reference failure strain are held constant. Therefore, the remainder of the paper will focus on the results obtained when the reference failure strain is held constant. That provides a constant baseline for the calculation of the hybrid effect, as the hybrid effect is calculated relative to that reference failure strain.

The influence of the glass fibre strength scatter is also investigated by varying the Weibull modulus, m_{GF}, while the reference composite failure strain is held constant. For these simulations, the reference values for the properties of carbon fibres are used. The results are summarised in Fig. 8a and b, demonstrating that the glass fibre strength scatter has a negligible influence on the hybrid effect. Some limited differences in the hybrid effect can be observed, but only at high hybrid volume fractions. This occurs only if the failure of the glass fibres commences at strains below the composite failure strain of the carbon fibres. Whether or not this occurs can be seen from the onset of deviation from linearity in the stress–strain diagrams in Fig. 8. Deviations from linearity indicate that significant fibre fracture is occurring. The softening of the glass fibre composite can partially overlap with the softening of the carbon fibre composite. If this occurs, then the hybrid effect will decrease.

3.3. Failure strain ratio

It is currently unclear from the literature whether the ratio of the failure strains of the two types of fibres is important in controlling the hybrid effect. As explained in Section 1, the conclusions of Fukuda (1984) and Zweben (1977) differed in this regard due to a different definition of the hybrid effect. In the GLS framework, the hybrid effect is clearly defined as the failure strain enhancement of the hybrid composite relative to the LE fibre reference composite. This enhancement is observed as a shift of the LE peak stress in the stress–strain curve to higher strains.

Due to the assumption of linear elasticity for the fibres, it is impossible to change the failure strain of the glass fibre reference composite, while keeping its stiffness and strength constant. Therefore, its strength is kept constant, while its stiffness and failure strain are varied. The glass fibre reference composite will be referred to as a HE composite in this section, as its stiffness will change. The results are shown in Fig. 9.

While the reference composite failure strain is increased from 5.33% to 8% and 20%, the HE fibre stiffness changed from 70 GPa, to 46.6 GPa and 18.6 GPa. The failure strain of the HE fibre composite should be compared to a failure strain of 3.18% for the carbon fibre reference composite. The increase in failure strain for the reference HE fibre composite seems to decrease the hybrid effect. It would be incorrect to conclude that the hybrid effect is inversely related to the ratio of the failure strains. Fig. 8b already indicated that the hybrid effect remains the same if the failure development of both fibre types does not overlap in strain. Therefore, it seems that decreasing the fibre stiffness has a more pronounced effect than the increased failure strain. The lower stiffness fibre is less efficient in sharing the load of the broken carbon fibres, leading to a larger fraction of the load shed to the intact carbon fibre fragments. This results in accelerated carbon fibre failure and a decreased hybrid effect.
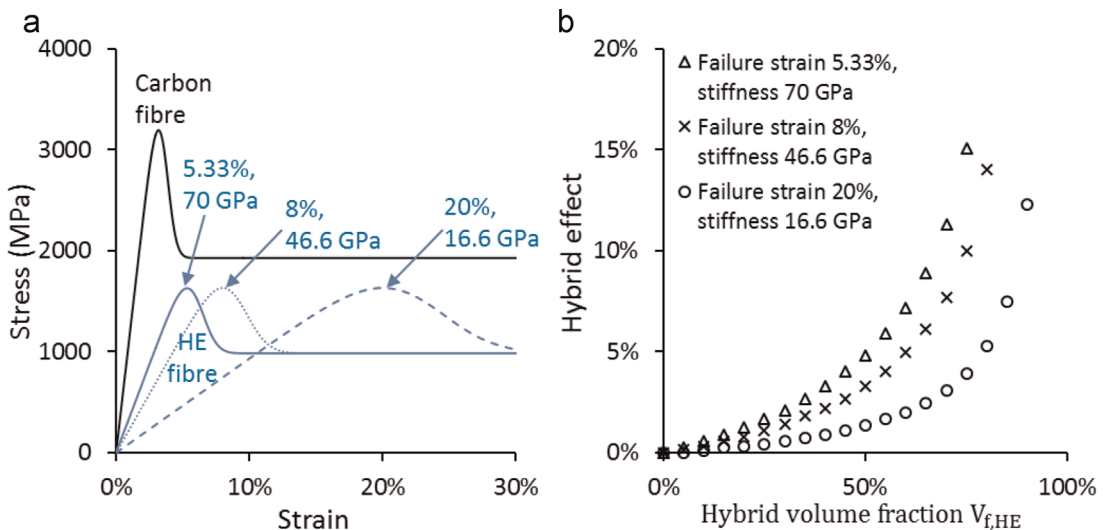

Fig. 9. (a) Stress–strain diagrams for a HE fibre composites with various HE failure strains and fibre stiffnesses, but the same tensile strength, and (b) its influence on the hybrid effect.
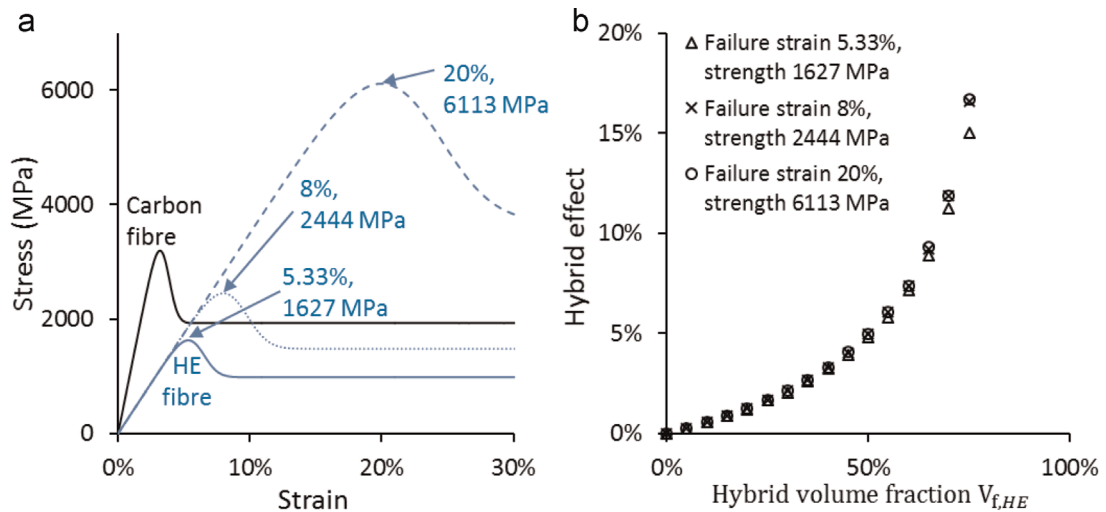
Fig. 10. (a) Stress–strain diagrams for a HE fibre composites with various HE failure strains and strengths but the same fibre tensile modulus, and (b) its influence on the hybrid effect.

As noted above, allowing the elastic modulus of the HE fibre to change while its failure strain is increased has unwanted side effects. To avoid this issue, the elastic modulus and Weibull modulus are kept constant for the HE fibres. The parameter $\sigma_{0,HE}$ and the strength of the reference HE fibre composite are varied to enable it to reach the required failure strains. The resulting stress–strain diagrams are shown in Fig. 10a.

Fig. 10b reveals that the failure strain of the HE composite only has a small influence on the hybrid effect if the HE fibre modulus remains the same. The only significant influence is found for the HE fibre composite with a 5.33% failure strain, which has a slightly lower hybrid effect at high hybrid volume fractions. In contrast with the results of Fukunaga et al. (1984), the GLS model does predict an influence of the failure strain ratio on the hybrid effect, albeit small. This is in line with the results of Zweben (1977). Zweben's definition of the hybrid effect was, however, based on the failure of the first HE fibre. This definition leads to an overestimation of the importance of this parameter. A more refined local load-sharing model for hybrid composites is expected to predict values in between Zweben's model and the GLS model.

The LE fibre break to cause stress concentrations on the HE fibre. The influence this has depends on the dispersion of both fibre types, which has been analysed in detail by Swolfs et al. (2015a). This influence is however small if the failure strains of both fibre types sufficiently far apart. This regime is the most important one, as it permits the largest hybrid effects as well as the largest improvements in ultimate failure strain, toughness and impact resistance.

4. Conclusion

A global load-sharing model for unidirectional fibre-reinforced hybrid composites is developed based on the fibre fragmentation model of Hui et al. (1995). This model predicts a hybrid effect in terms of failure strain of up to 15% for carbon/glass hybrids. These hybrid effects correspond well to the available experimental data. The carbon fibre strength scatter is shown to be a crucial parameter in determining the hybrid effect for failure strain. The glass fibre strength scatter is not important, as long as the failure of the two fibre types occurs in different strain intervals. The failure strain ratio of the two fibre types has only a small influence. A non-dimensional analysis showed that the hybrid effect is influenced by only 4 parameters: the Weibull moduli of the LE and HE fibres and two non-dimensional parameters. For LE Weibull moduli of 5 or higher, the hybrid effect only depends on the LE Weibull modulus and the ratio of fibre stiffness times the relative volume fraction of the LE and HE composites.

These new insights into the hybrid effect now need to be verified in a local load-sharing model. This will allow the local effects to be analysed, which is impossible in a global load-sharing model. Local load-sharing models are crucial to obtain quantitative predictions of the hybrid effect and to allow a wider applicability of hybrid composites.

Acknowledgements

Appendix. Fibre fragmentation solution

The dimensionless fragment length ℓ is defined as the fragment length divided by δ_{char}. The model accounts for three fragment length regimes, characterised by the strain ranges: $\ell < \Delta/2$, $\Delta/2 < \ell < \Delta$, and $\ell > \Delta$. Under the assumption of constant shear stress in the matrix, the probability of these three regimes can be calculated as a function of the normalised strain. The average normalised stress can then be calculated as a function of normalised strain:

$$S(\Delta) = \int_0^{\Delta/2} \frac{\ell^2}{2} p_1(\Delta, \ell) d\ell + \int_{\Delta/2}^{\Delta} \frac{\ell^2}{2} p_2(\Delta, \ell) d\ell + \int_{\Delta}^{\infty} \left[(\ell - \Delta)\Delta + \frac{\Delta^2}{2} \right] p_3(\Delta, \ell) d\ell$$

(A.1)

The three integrals are related to the three fragment length regimes. The functions $p_i(\Delta, \ell)$ represent the probability densities of those fragments and can be calculated by

$$p_1(\Delta, \ell) = p(\ell) + 2m \int_{\ell}^{2\ell} \frac{A_0(t)}{t} \exp\left[-t^m \left(\ell + \frac{t}{2} \right) \right] dt,$$

(A.2)

$$p_2(\Delta, \ell) = p(\ell) + 2m \int_{\ell}^{\Delta} \frac{A_0(t)}{t} \exp\left[-t^m \left(\ell + \frac{t}{2} \right) \right] dt,$$

(A.3)

$$p_3(\Delta, \ell) = A_0(\Delta) \exp\left(-\Delta^m \ell \right),$$

(A.4)

where

$$p(\ell) = \ell^{2m} \exp\left(\frac{-\ell^{m+1}}{m+1} \right) \psi\left(\frac{\ell^{m+1}}{2} \right),$$

(A.5)

$$A_0(\ell) = \ell^{2m} \exp\left(\frac{m\ell^{m+1}}{m+1} \right) \psi\left(\frac{\ell^{m+1}}{2} \right)$$

(A.6)

and

$$\psi(x) = \exp\left(\frac{-2m}{m+1} \int_0^x \frac{1 - \exp(-t)}{t} dt \right).$$

(A.7)

The entire procedure was implemented in Mathworks' Matlab R2013b. Fig. A.1 depicts the flow chart of the calculations.
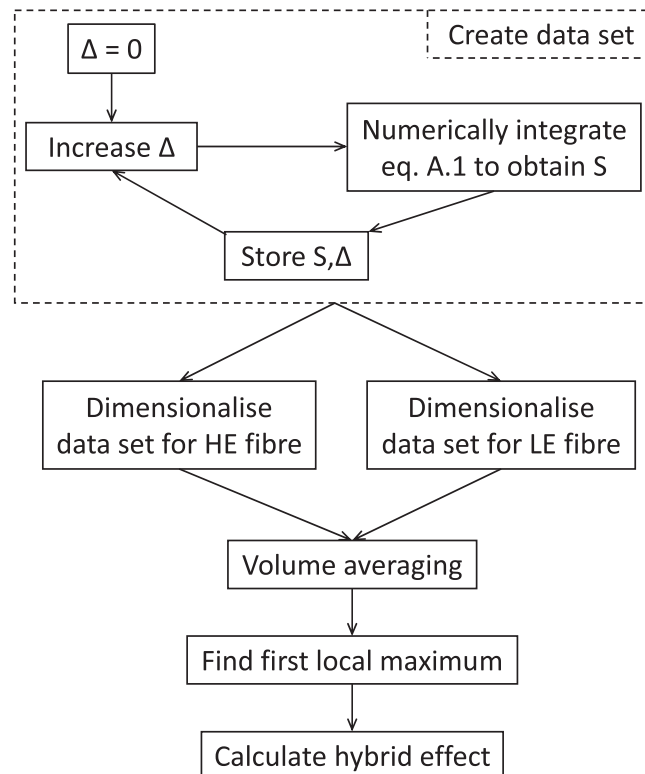

Fig. A.1. Flow chart of the GLS model for hybrid composites.

All integrals were numerically evaluated using adaptive Simpson quadrature. The non-dimensional solutions to these equations were accurately evaluated for a wide range of strains. These solutions were saved as a data set, so that they can be efficiently used for hybrid composites. The data set is dimensionalised to calculate the hybrid stress–strain diagrams without having to re-run the solution to Hui's model. The model then searches for the strain at the first local maximum, and compares this to the failure strain of the LE composite to calculate the hybrid effect.

References

Behzadi, S., Curtis, P.T., Jones, F.R., 2009. Improving the prediction of tensile failure in unidirectional fibre composites by introducing matrix shear yielding. Compos. Sci. Technol. 69, 2421–2427.

Callens, M.G., Gorbatikh, L., Verpoest, I., 2014. Ductile steel fibre composites with brittle and ductile matrices. Compos. Part A: Appl. Sci. Manuf. 61, 235–244.

Curtin, W.A., 1991a. Exact theory of fibre fragmentation in a single-filament composite. J. Mater. Sci. 26, 5239–5253.

Curtin, W.A., 1991b. Theory of mechanical properties of ceramic–matrix composites. J. Am. Ceram. Soc. 74, 2837–2845.

Curtin, W.A., 2000. Tensile strength of fiber-reinforced composites: III. Beyond the traditional Weibull model for fiber strengths. J. Compos. Mater. 34, 1301–1332.

Czél, G., Wisnom, M.R., 2013. Demonstration of pseudo-ductility in high performance glass/epoxy composites by hybridisation with thin-ply carbon prepreg. Compos. Part A: Appl. Sci. Manuf. 52, 23–30.

Dai, G., Mishnaevsky Jr., L., 2014. Fatigue of hybrid glass/carbon composites: 3D computational studies. Compos. Sci. Technol. 94, 71–79.

de Morais, A.B., 2006. Prediction of the longitudinal tensile strength of polymer matrix composites. Compos. Sci. Technol. 66, 2990–2996.

Diao, H., Bismarck, A., Robinson, P., Wisnom, M.R., 2012. Pseudo-ductile behaviour of unidirectional fibre reinforced polyamide 12 composite by intra-tow hybridization. In: Proceedings of the 15th European Conference on Composite Materials, Venice.

Fukuda, H., 1984. An advanced theory of the strength of hybrid composites. J. Mater. Sci. 19, 974–982.

Fukunaga, H., Tsu-Wei, C., Fukuda, H., 1984. Strength of intermingled hybrid composites. J. Reinf. Plast. Compos. 3, 145–160.

Harlow, D.G., 1983. Statistical properties of hybrid composites. I. Recursion analysis. Proc. R. Soc. Lond. Ser. A: Math. Phys. Eng. Sci. 389, 67–100.

Hayashi, T., 1972. On the improvement of mechanical properties of composites by hybrid composition. In: Proceedings of the 8th International Reinforced Plastics Conference, pp. 149–152.

Hine, P.J., Bonner, M., Ward, I.M., Swolfs, Y., Verpoest, I., Mierzwa, A., 2014. Hybrid carbon fibre/nylon 12 single polymer composites. Compos. Part A: Appl. Sci. Manuf. 65, 19–26.

Hui, C.Y., Phoenix, S.L., Ibnabdeljalil, M., Smith, R.L., 1995. An exact closed form solution for fragmentation of Weibull fibers in a single filament composite with applications to fiber-reinforced ceramics. J. Mech. Phys. Solids 43, 1551–1585.

Ibnabdeljalil, M., Curtin, W.A., 1997. Strength and reliability of fiber-reinforced composites: localized load-sharing and associated size effects. Int. J. Solids Struct. 34, 2649–2668.

Kretsis, G., 1987. A review of the tensile, compressive, flexural and shear properties of hybrid fibre-reinforced plastics. Composites 18, 13–23.

Landis, C.M., McMeeking, R.M., 1999. A shear-lag model for a broken fiber embedded in a composite with a ductile matrix. Compos. Sci. Technol. 59, 447–457.

Manders, P.W., Bader, M.G., 1981. The strength of hybrid glass/carbon fibre composites Part 1 Failure strain enhancement and failure mode. J. Mater. Sci. 16, 2233–2245.

Naito, K., Tanaka, Y., Yang, J.-M., Kagawa, Y., 2008. Tensile properties of ultrahigh strength PAN-based, ultrahigh modulus pitch-based and high ductility pitch-based carbon fibers. Carbon 46, 189–195.

Nedele, M.R., Wisnom, M.R., 1994. Three-dimensional finite element analysis of the stress concentration at a single fibre break. Compos. Sci. Technol. 51, 517–524.

Neumeister, J.M., 1993a. Bundle pullout—a failure mechanism limiting the tensile strength of continuous fiber reinforced brittle matrix composites—and its implications for strength dependence on volume and type of loading. J. Mech. Phys. Solids 41, 1405–1424.

Neumeister, J.M., 1993b. A constitutive law for continuous fiber reinforced brittle matrix composites with fiber fragmentation and stress recovery. J. Mech. Phys. Solids 41, 1383–1404.

Peijs, A., Catsman, P., Govaert, L.E., Lemstra, P.J., 1990. Hybrid composites based on polyethylene and carbon fibres Part 2: Influence of composition and adhesion level of polyethylene fibers on mechanical properties. Composites 21, 513–521.

Perry, J.L., Adams, D.F., 1975. Charpy impact experiments on graphite/epoxy hybrid composites. Composites 6, 166–172.

Phillips, L.N., 1976. The hybrid effect – does it exist? Composites 7, 7–8.

Phoenix, S.L., 1974. Probabilistic strength analysis of fibre bundle structures. Fibre Sci. Technol. 7, 15–31.

Phoenix, S.L., Ibnabdeljalil, M., Hui, C.Y., 1997. Size effects in the distribution for strength of brittle matrix fibrous composites. Int. J. Solids Struct. 34, 545–568.

Pimenta, S., Pinho, S.T., 2013. Hierarchical scaling law for the strength of composite fibre bundles. J. Mech. Phys. Solids 61, 1337–1356.

Rajan, V.P., Zok, F.W., 2012. Effects of non-uniform strains on tensile fracture of fiber-reinforced ceramic composites. J. Mech. Phys. Solids 60, 2003–2018.

Rosen, B.W., 1964. Tensile failure of fibrous composites. AIAA J. 2, 1985–1991.

Scott, A.E., Sinclair, I., Spearing, S.M., Thionnet, A., Bunsell, A.R., 2012. Damage accumulation in a carbon/epoxy composite: comparison between a multiscale model and computed tomography experimental results. Compos. Part A: Appl. Sci. Manuf. 43, 1514–1522.

Shan, Y., Liao, K., 2002. Environmental fatigue behavior and life prediction of unidirectional glass–carbon/epoxy hybrid composites. Int. J. Fatigue 24, 847–859.

Swolfs, Y., Crauwels, L., Gorbatikh, L., Verpoest, I., 2013a. The influence of weave architecture on the mechanical properties of self-reinforced polypropylene. Compos. Part A: Appl. Sci. Manuf. 53, 129–136.

Swolfs, Y., Crauwels, L., Van Breda, E., Gorbatikh, L., Hine, P., Ward, I., Verpoest, I., 2014a. Tensile behaviour of intralayer hybrid composites of carbon fibre and self-reinforced polypropylene. Compos. Part A: Appl. Sci. Manufacturing 59, 78–84.

Swolfs, Y., Gorbatikh, L., Romanov, V., Orlova, S., Lomov, S.V., Verpoest, I., 2013b. Stress concentrations in an impregnated fibre bundle with random fibre packing. Compos. Sci. Technol. 74, 113–120.

Swolfs, Y., Gorbatikh, L., Verpoest, I., 2013c. Stress concentrations in hybrid unidirectional fibre-reinforced composites with random fibre packings. Compos. Sci. Technol. 85, 10–16.

Swolfs, Y., Gorbatikh, L., Verpoest, I., 2014b. Fibre hybridisation in polymer composites: a review. Compos. Part A: Appl. Sci. Manuf. 67, 181–200.

Swolfs, Y., McMeeking, R.M., Gorbatikh, L., Verpoest, I., 2015a. The effect of fibre dispersion on initial failure strain and cluster development in unidirectional carbon/glass hybrid composites. Compos. Part A: Appl. Sci. Manuf. 69, 279–287.

Swolfs, Y., McMeeking, R.M., Verpoest, I., Gorbatikh, L., 2015b. Matrix cracks around fibre breaks and their effect on stress redistribution and failure development in unidirectional composites. Compos. Sci. Technol. 108, 16–22.

Swolfs, Y., Van den fonteyne, W., Baets, J., Verpoest, I., 2014c. Failure behaviour of self-reinforced polypropylene at and below room temperature. Compos. Part A: Appl. Sci. Manuf. 65, 100–107.

Swolfs, Y., Verpoest, I., Gorbatikh, L., 2015c. Issues in strength models for unidirectional fibre-reinforced composites. Compos. Sci. Technol. 114, 2015, 42-49.

Swolfs, Y., Morton, H., Scott, A.E., Gorbatikh, L., Reed, P.A.S., Sinclair, I., Spearing, S.M., Verpoest, I., 2015d. Synchrotron radiation computed tomography for experimental validation of a tensile strength model for unidirectional fibre-reinforced composites. Compos. Part A: Appl. Sci. Manuf. 77, 106–113.

Swolfs, Y., Zhang, Q., Baets, J., Verpoest, I., 2014d. The influence of process parameters on the properties of hot compacted self-reinforced polypropylene composites. Compos. Part A: Appl. Sci. Manuf. 65, 38–46.

Taketa, I., Ustarroz, J., Gorbatikh, L., Lomov, S.V., Verpoest, I., 2010. Interply hybrid composites with carbon fiber reinforced polypropylene and self-reinforced polypropylene. Compos. Part A: Appl. Sci. Manuf. 41, 927–932.

Thomason, J.L., 2013. On the application of Weibull analysis to experimentally determined single fibre strength distributions. Compos. Sci. Technol. 77, 74–80.

Verpoest, I., Lomov, S., Swolfs, Y., Jacquet, P., Michaud, V., Manson, J.-A., Hobdell, J., Hine, P., Marquette, P., Herten, H., Vasiliadis, H., 2014. Advanced materials enabling high-volume road transport applications of lightweight structural composite parts. Sampe J. 50, 30–37.

Wang, F., Chen, Z.Q., Wei, Y.Q., Zeng, X.G., 2010. Numerical modeling of tensile behavior of fiber-reinforced polymer composites. J. Compos. Mater. 44, 2325–2340.

Watanabe, J., Tanaka, F., Okabe, T., 2013. The tensile strength distribution of carbon fibers at short gauge length. In: Proceedings of the 38th Conference of the Japan Society for Composite Materials, pp. 171–172.

Watanabe, J., Tanaka, F., Okuda, H., Okabe, T., 2014. Tensile strength distribution of carbon fibers at short gauge lengths. Adv. Compos. Mater., 1–16.

Xing, J., Hsiao, G.C., Chou, T.W., 1981. A dynamic explanation of the hybrid effect. J. Compos. Mater. 15, 443–461.

You, Y.J., Park, Y.H., Kim, H.Y., Park, J.S., 2007. Hybrid effect on tensile properties of FRP rods with various material compositions. Compos. Struct. 80, 117–122.

Zeng, Q.D., 1994. A statistical analysis of the tensile failure and hybrid effect of an intraply hybrid composite. Int. J. Fract. 68, 351–362.

Zweben, C., 1977. Tensile strength of hybrid composites. J. Mater. Sci. 12, 1325–1337.